Paper accepted for presentation at 2009 IEEE Bucharest Power Tech Conference, June 28th - July 2nd, Bucharest, Romania

Measurements and Computation of Electromagnetic Field in Transformer Station 400/110 kV Ernestinovo

S. Nikolovski, *Senior Member, IEEE*, Z. Klaić, B. Štefić

***Abstract*—This paper presents results of measurements and computations of the electric and magnetic fields of complex busbars, transformers and transmission line structures at transformer station 400/110 kV. The fundamental sources of low frequency electromagnetic fields in the transformer station are the primary elements of the 400 and 110 kV open substations and associated overhead lines. Due to the complexity of the geometry of the substation elements, it was necessary to apply a three-dimensional approach to the computation of the electromagnetic field. Measurements were performed by EMS 100 field meter and computations of electromagnetic fields were conducted for quasi-static states of electrical values at a power frequency of 50 Hz. The calculated electric and magnetic fields were compared with measured values and permissible levels according to Croatian regulations. Measurements were performed for real working conditions for twelve different profiles in the transformer station.**

***Keywords*—Transformer station, electric field, magnetic filed, electromagnetic compatibility, measurements**

I. Introduction

A rebuilt transformer station 400/110/ kV is in operation for more than two years and according to the Law on Non-Ionizing Radiation Protection of Croatia there is an official demand from HEP TSO for measurements of electric and magnetic fields on site within the fence of the transformer station. The fundamental sources of low frequency electromagnetic fields in the TS 400 kV are the primary elements of 400 kV and 110 kV open substations as well as connected 400 and 110 kV overhead lines. Due to the complexity of the geometry of the above mentioned elements, it is necessary to apply a three-dimensional approach to the computations of the electromagnetic field. Measurements of electromagnetic fields were performed for 12 profiles and computations were conducted for quasi-static states of electrical values at the frequency of 50 Hz.

The equipment within the transformer station 400/110/ kV generates a permanent 50 Hz electromagnetic field. Consequently, we have the following limiting levels of electric field intensity *E* and magnetic flux density *B:*

This work was supported in part by the HEP Croatian National Grid Company.

S. Nikolovski and Z. Klaić are with Faculty of Electrical Engineering, J.J. Strossmayer University of Osijek, 31000 CROATIA (e-mail: srete@etfos.hr).

B. Štefić is with HEP Croatian National Grid Company, 10000 Zagreb CROATIA (e-mail: branko.stefic@hep.org).

- for the field of professional exposure (8 hrs/day) E_{g8h} = 5000 V/m and B_{g8h}= 100 μT
- for the field of enhanced sensitivity (24 hrs/day) E_{g24h} = 2000 V/m and B_{g8h}= 40 μT

II. Theoretical Model of Emf

The computations presented in this paper were carried out with the HIFREQ [6,7] program of the CDEGS [8] software package. This program calculates the current distribution in conductor networks consisting of rectilinear segments, and uses this current distribution to compute the potential, electric field and magnetic field at selected points in space. The program can account for the presence of multiple horizontal layers of soil with different electrical characteristics. The conductors and observation points (i.e. the points where the potential and electromagnetic fields are computed) can be located in the air or in any of the earth layers.

The methodology used in the program is described in detail in References 6 and 7. A brief summary is presented below. The potential and electromagnetic fields are first expressed in terms of the components of a vector potential, which is in turn expressed as a function of the currents flowing in each segment of the conductor network. The currents in the conductor segments are determined by the requirement that the voltage drop between pairs of points in the network be equal to the *ZI* drop along a path connecting the points:

$$\int_{P_1}^{P_2} \vec{E} \cdot d\vec{l} - \int_{P_1}^{P_2} ZI \; dl = 0 \qquad (1)$$

Here, *Z* is the internal impedance of the conductor and *I* the current flowing in it. Points P_1 and P_2 are normally taken as the mid-points of adjacent segments and the integrals are carried out over the shortest path linking them.

This technique (which is a special application of the method of moments) fully accounts for mutual interactions (conductive, capacitive and inductive) between the conductor segments, and also accounts for the potential drop along the conductors due to their self-impedance.

A. Computation of the Conservative Electric Field

While calculating the conservative electric field, only conductors which are at known potentials are taken into consideration. Furthermore, as the charges are located at the surface of the conductors, it is necessary to distribute the charges appropriately on the conductor surface, which

978-1-4244-2235-7/09/$25.00 ©2009 IEEE

is later easily, associated with the appropriate mathematical tool with field equation. The conductor surface was modeled with a thin one-dimensional wire grid. The effect of permittivity discontinuity (ε) on the ground-air interface, i.e. the effect of ground on the electric conductor potential, was taken into consideration by using the mirror technique. The phasor of the electric potential $\dot{\varphi}(\vec{r})$ located at some point in space can be obtained by applying the superposition theorem as an infinite sum of potentials caused by elementary time variable charges $d\dot{q} = \dot{\lambda}(\vec{r}')dl'$ on the conductor surface. The infinite sum is treated as an integral for the electric potential $\dot{\varphi}(\vec{r})$ caused by line charge density $\dot{\lambda}(\vec{r}')$, which is located at a point given by the position vector $\vec{r}'$ placed on all thin wire parts (structures), including the original conductors and their images with respect to the ground-air discontinuity, and is given by the following integral equation:

$$\dot{\varphi} = \frac{1}{4\pi\varepsilon}\int_{l'}\frac{\dot{\lambda}(\vec{r}')dl'}{|\vec{r}-\vec{r}'|} + \frac{1}{4\pi\varepsilon}\int_{l'}\frac{\dot{\lambda}(\vec{r}'')dl''}{|\vec{r}-\vec{r}''|} \tag{2}$$

where:

$\dot{\lambda}(\vec{r}')$ - phasor of line charge density of the original conductor [A/m],

$\dot{\lambda}(\vec{r}'')$ - phasor of line charge density of the mirrored conductor [A/m],

$|\vec{r}-\vec{r}'|$ - distance between the observation point and the phasor of line charge density of the original conductor [m],

$|\vec{r}-\vec{r}''|$ - distance between the observation point and the phasor of line charge density of the mirrored conductor [m],

ε -permittivity of space in which the field is calculated, i.e. for air follows $\varepsilon = \varepsilon_0$,

l', l'' - integration on the original (mirrored) conductor

Since the line charge density appearing under the integral sign is an unknown function, expression (1) has to be solved using a numerical method due to the lack of a more appropriate analytical expression. In this paper, the moment method (MOM), which has proven to be effective when solving electromagnetic tasks in unlimited space, was used for solving the equation (1). In order to use the moment method for solving the equation (1), it is necessary to perform a discretization of this equation. This is performed through the discretization of an unknown distribution of field source i.e. line charge density $\dot{\lambda}(\vec{r}')$ by using a combination of appropriate number of *N* linearly independent fundamental functions. Thereupon, the discretization of conductor length on N segments and the discretization of observation points will be conducted. First, it is necessary to divide the conductors into segments of finite lengths Δl (j=1, N), which can be a line or ring depending on the desired accuracy. Then, it is necessary to approximate the unknown distribution of field source with the appropriate number of fundamental functions λ_j in the form of the following expression:

$$\dot{\lambda} = \sum_{j=1}^{N} a_j'\lambda_j' \text{ that is } \dot{\lambda} = \sum_{j=1}^{N} a_j''\lambda_j'' \tag{3}$$

where:

λ_j' - fundamental function on segment j of the original conductor,

λ_j'' - fundamental function on segment j of the mirrored conductor.

A constant on the segment has been chosen, and $a_j' = 1$ is on the observed segment, whereas it is zero on other segments. The same goes for a_j''. Taking into consideration that the constant on the segment has been chosen as the fundamental function and that great accuracy is required, the number of segments per conductor has been increased so that the longest segment length does not exceed the length of 1 m. Based on the above discussion, expression (1) can be written as:

$$\dot{\varphi}(\vec{r}) = \frac{1}{4\pi\varepsilon}\sum_{j=1}^{N}\int_{\Delta l_j'}\frac{a_j'\lambda_j'(\vec{r}')dl'}{|\vec{r}-\vec{r}'|} + \frac{1}{4\pi\varepsilon}\sum_{j=1}^{N}\int_{\Delta l_j''}\frac{a_j''\lambda_j''(\vec{r}'')dl''}{|\vec{r}-\vec{r}''|} \tag{4}$$

Since $\lambda' = -\lambda''$, it is obvious that the expression (3) has N unknowns on the right side. In order to solve the expression, N observation points in space where the potential is known and which corresponds to the conductors under voltage have to be chosen. Thus, the system of *N* equations with *N* unknowns is obtained, which is determined in matrix form as

$$[\varphi] = [p][\lambda] \tag{5}$$

where the elements $p_{i,j}$ of the matrix system [p] represent the potential at observation point "i", i.e. observed point placed on the conductor surface of line current density λ_j.

The Gauss-Seidel iterative method was used for solving the matrix equation. In this process, the iteration was considered successful the moment a relative accuracy of 10^{-7} was reached. Once equation (4) has been solved, i.e. an approximation of the line current density on the conductors has been obtained; the vector-phasor of the conservative component of electric field intensity on the observation point with a position vector $\vec{r}$ can be determined by using the following equation (6).

$$\dot{\vec{E}}(\vec{r}) = \frac{1}{4\pi\varepsilon}\sum_{j=1}^{N}\int_{\Delta l_j'}\frac{a_j'\lambda_j'(\vec{r}')(\vec{r}-\vec{r}')dl'}{|\vec{r}-\vec{r}'|^3} + \frac{1}{4\pi\varepsilon}\sum_{j=1}^{N}\int_{\Delta l_j''}\frac{a_j''\lambda_j''(\vec{r}'')(\vec{r}-\vec{r}'')dl''}{|\vec{r}-\vec{r}''|^3} \tag{6}$$

Considering that a three-dimensional computation of electric field intensity vector, which is caused by line charge density of a three-phase system that are mutually

phase shifted by 120° and at the same time spatially displaced (space between phases), is being required, it should be taken into account that electric field intensity is elliptically polarized at every point in space. In other words, the peak of electric field intensity in time traces an ellipse as shown in Fig.1.

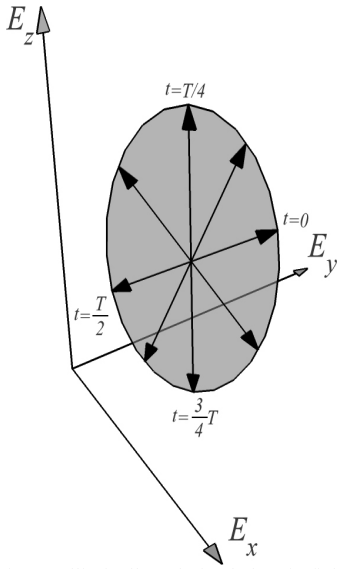

Fig. 1 Elliptically polarized electric field

Since each of the three components of the electric field have a different sum and phase shift, the following can be applied:

$$E_x(t) = E_{x,\max}\sin(314t+\varphi_x),$$
$$E_y(t) = E_{y,\max}\sin(314t+\varphi_y), \quad (7)$$
$$E_z(t) = E_{z,\max}\sin(314t+\varphi_z).$$

The absolute value of the electric field intensity vector, is defined by the following expression

$$E(t) = \sqrt{E_x^2(t)+E_y^2(t)+E_z^2(t)} \quad (8)$$

whereas the RMS value of absolute value of electric field intensity is defined by the following expression:

$$E = \sqrt{\frac{E_{x,\max}^2}{2}+\frac{E_{y,\max}^2}{2}+\frac{E_{z,\max}^2}{2}} \quad (9)$$

B. Computation of the MagneticField Density

Space in air where the rotational component of the EMF was computed, has been modeled as a linear isotropic half-space having the same properties as a vacuum i.e. $\varepsilon=\varepsilon_0, \mu=\mu_0, \kappa=0$. Discontinuity of these properties arises on the plane separating ground and air, which is defined by the coordinate z = 0. The electric properties of the half-space below the limiting ground-air plane are defined by the soil characteristics $\varepsilon_r \approx 80, \mu=\mu_0$ and $\kappa=0.01$ S/m. The magnetic field in the observed part of the half-space is defined as

$$\vec{B} = \frac{\mu_0}{4\pi}\int_{l_j}\frac{\dot{I}d\vec{l}\times(\vec{r}-\vec{r}')}{|\vec{r}-\vec{r}'|} \quad (10)$$

Both expressions (1) and (10) are discretized, i.e. the integral is calculated as the sum of effects of all conductor segments at the observation point. The electromagnetic field is determined at points located at the nodes of a rectangular grid with equal mesh size at a height of 2 m above the ground, which lies in the x-y plane, i.e. parallel to the plane separating ground from air. The space between two consecutive observation points in the *x* and *y* directions is 2m.

III. Computation of the Electric Field

A graphical model of TS 400/110 kV used for the computation of electric field is shown in Fig. 4, as modeled in the HIFREQ module of the CDEGS software. While computing the conservative electric field, the phase voltages of a three-phase balanced system were imposed on the conductors.

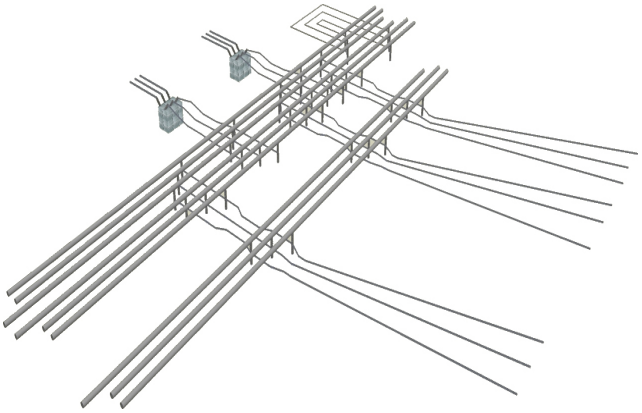

Fig. 2 Physical model of TS 400/110 kV used for computing the electric field

The phase voltages of the conductors in the part of the substation operated at 400 kV are:

$\varphi_A = 238584\, e^{j0}$ V; $\varphi_B = 238584\, e^{j240}$ V; $\varphi = 238584\, e^{j120}$ V

The phase voltages of the conductors in the part of the substation operated at 110 kV are:

$\varphi_A = 63584\, e^{j0}$ V; $\varphi_B = 63584\, e^{j240}$ V; $\varphi_C = 63584\, e^{j120}$ V

The subject of this analysis is a long-term (eight-hour or twenty four-hour) exposure of people to the electric field. Consequently, the field of the balanced voltage system has been calculated.

C. Electric Field Intensity Inside TS 400/110 kV

The spatial distribution of the electric field for twelve profiles are measured and computed inside TS 400/110 kV. Profiles were chosen by HEP TSO engineers for several interesting profiles of 400 kV facilities and two profiles on 110 kV side. In Fig. 5, measured points on twelve profiles are presented. All computations have been conducted for the surface located 1,5 m above the ground.

Measured points are arranged in 12 profiles:

1. C0-1 the middle of the merge field of two 400 kV busbars
2. C3-4 is under double busbars system and 400 kV line Mitrovica
3. C4-5 is under double busbars system and auxiliary busbars and 400 kV line Ugljevik
4. C7-8 is under double busbars system and in direction of T2 transformer
5. C8-9 is under double busbars system and in the middle of 400 kV line Ugljevik
6. C9-10 is under double busbars system and left of 400 kV line Ugljevik
7. T1/400 and T2/400 are under busbars which connect transformers on the main 400 kV busbars system
8. T1/110 and T2/110 are under busbar which connect transformers on the main 110 kV busbar system
9. UPS is under left side of 400 kV line perpendicular to the line direction
10. UOG is under left side of 400 kV near the fence inside the substation

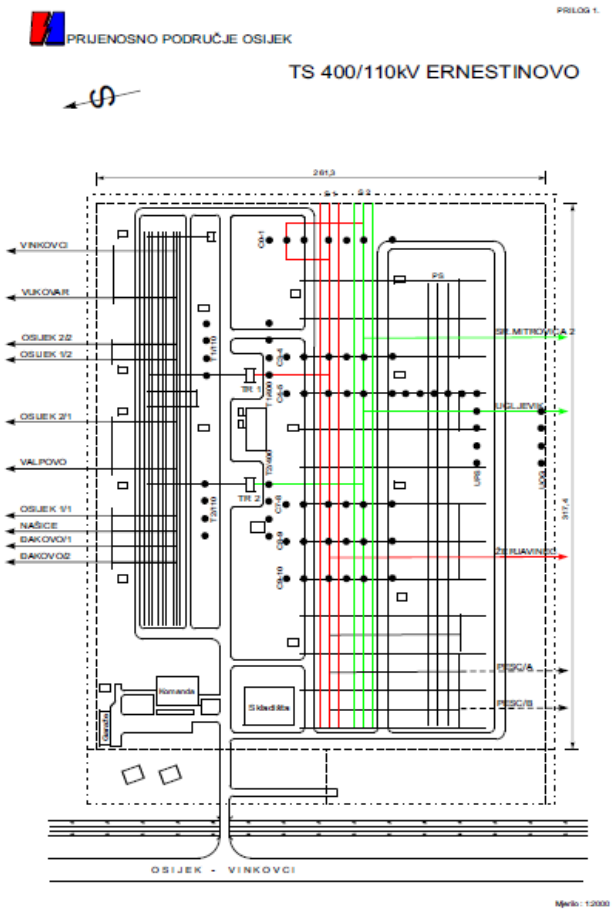

Fig. 2 Disposition of measured points in 400/110 kV transformer station

Due to the lack of space in the paper, only several measurements and computed profiles will be presented. In Fig. 2, monitoring points for all 12 profiles are presented. The Maschek EMS-100 fieldmeter is used for measurements of electric and magnetic fields.
Measured results at profile C01are presented in Table 1.

Table 1 Electric field at profile **C 0-1**

Time	Date	H-Field X [nT]	H-Field Y [nT]	H-Field Z [nT]	H-Field 3D [nT]
10:49	15.7.2008	522,5	3155	3800	4966,59
10:51	15.7.2008	633	2380	2560	3552,28
10:53	15.7.2008	2475	2245	2310	4062,23
10:53	15.7.2008	7620	3160	2105	8513,58
10:54	15.7.2008	7760	3655	2240	8865,34
10:55	15.7.2008	6240	4120	2325	7830,56
10:56	15.7.2008	3165	770,5	1717	3682,25

Table 2 Magnetic field at profile **C 0-1**

E-Field X [V/m]	E-Field Y [V/m]	E-Field Z [V/m]	E-Field 3D [V/m]
275	8865	4570	9977,41
762	8905	8585	12392,82
362,5	9460	10080	13828,57
1765	3975	5540	7043,26
1685	3495	2980	4892,31
1530	5255	3755	6637,47
526,5	3820	4325	5794,41

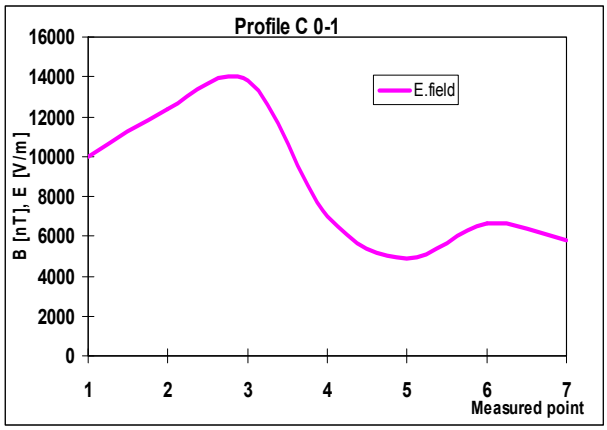

Fig. 3 Measured values for E-field at profile C0-1

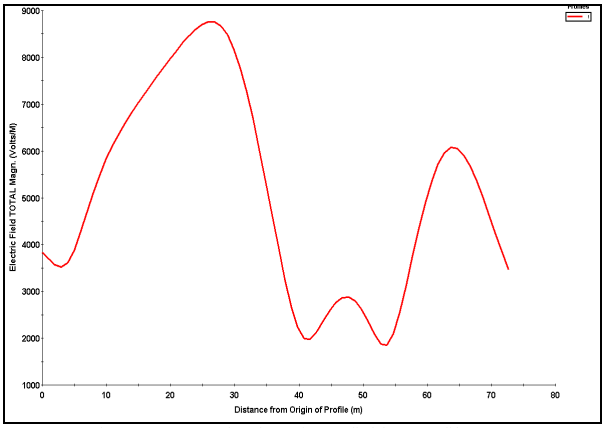

Fig. 4 Computed values for E-field at profile C0-1

In Fig. 3 and 4 can be seen that the shape of the measured and computed values of electric field at profile C01 are similar. Difference in electric filed magnitude exists because of the influence of different metallic structures for frames for busbars, current, voltage transformers, breakers, disconnectors, etc. The model in the computer program is simplified.

Table 3 Measurements of electric and magnetic field at profile C 3-4

Time	H-Field 3D [nT]	E-Field 3D [V/m]
9:51:28	3767,03	4561,89
9:52:16	3933,62	6037,96
9:53:24	4383,78	4953,24
9:54:17	3417,48	5674,04
9:55:42	2342,99	7237,47
9:58:11	2109,37	11055,39
10:04:31	1060,16	9821,55

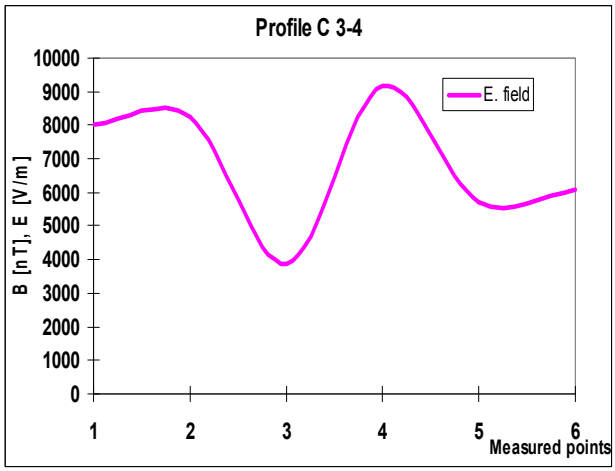

Fig. 5 Measured values for E-field at profile C3-4

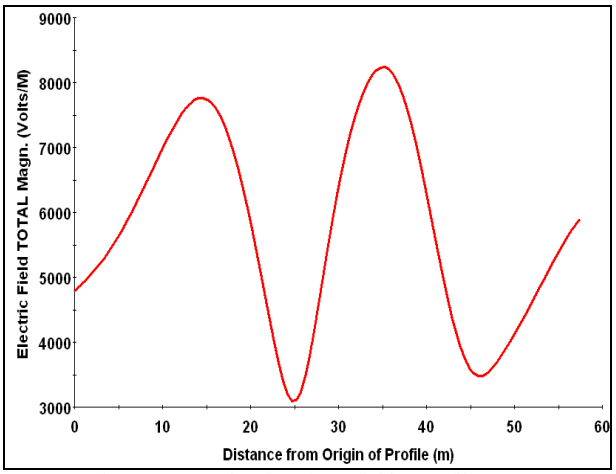

Fig. 6 Computed values for E-field at profile C3-4

Table 4 Measurements of electric and magnetic field at profile C9-10

Time	H-Field 3D [nT]	E-Field 3D [V/m]
11:26	407,27	3826,8
11:27	493,53	4714,18
11:27	1381,6	2469,13
11:28	4681,11	11804,21
11:29	4990,61	7323,68
11:30	4645,03	6292,32

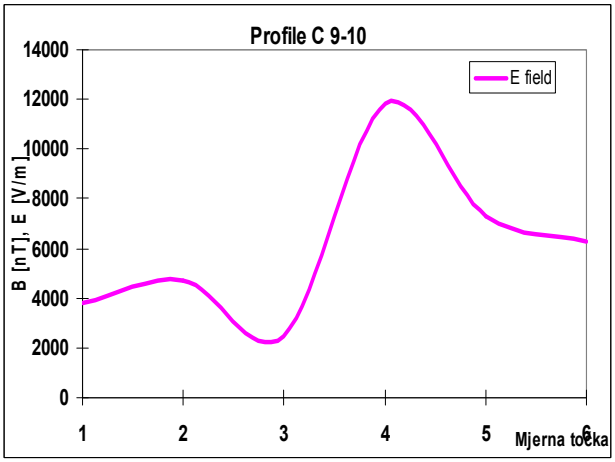

Fig. 7 Measured values for E-field at profile C9-10

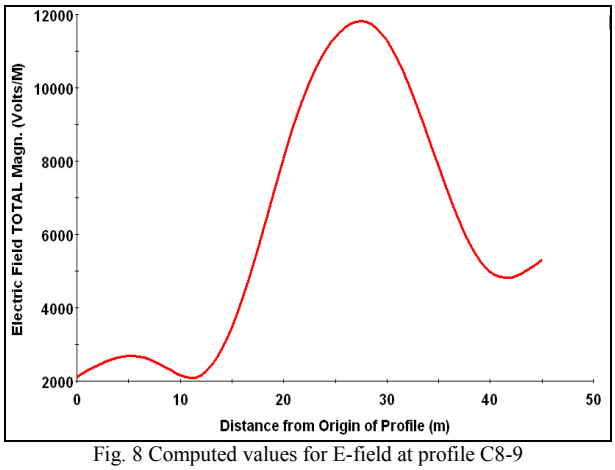

Fig. 8 Computed values for E-field at profile C8-9

For profile C9-10, the computed and measured amplitude of E field are close to each other.

Computed values for the whole profile which is 2 m over ground shows that permissible levels for E – field were reached inside the transformer station in area colored by green, yellow and red.

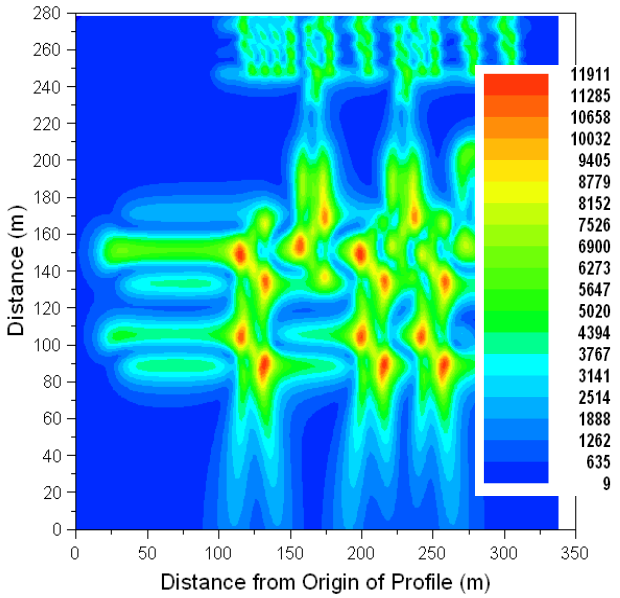

Fig. 9 Computed values for E-field on the whole plane

IV. Computation of the Magnetic Field

D. Input Data

Computation of the magnetic field cannot be accurately specified due to the impossibility to predict the currents flowing through the conductors at a given moment. Only severe seasonal and daily load variations can be predicted. Unbalances occurring at the 400 kV and 110 kV level can be disregarded so that the transmission lines, power transformers and other parts of the substation are considered to be loaded by a balanced system of phase the currents. The basic technical and measurement data are taken from the measuring system of TS 400/110 kV transformer station dispatching center. Fig. 10 presents current distribution at the time when the measurements of electric (E) and magnetic (H) field were performed.

- Transmission line 400 kV :
  TL Ernestinovo-Žerjavinec (Al/Fe 2x490/65 mm^2), phase currents are: I_1=156A $\angle 0^o$ I_2 = -76+j135 A, I_3 =-76-j135 A
  TL Ernestinovo-Ugljevik (Al/Fe 2x490/65 mm^2), phase currents are: I_1=50A $\angle 0^o$ I_2= -25.18+j43.61A, I_3 =-25.18-j43.61A
  TL Ernestinovo.-Mladost (Al/Fe 2x490/65 mm^2), phase currents are: I_1=350A $\angle 0^o$ I_2= -175+j303 A, I_3 =-175-j303 A

- Power transformers :
  Trafo 400/110 kV, rated power 300 MVA, primary phase currents are I_{pr1} = 184 A $\angle 0^o$ I_{pr2} = 184 A $\angle 120^o$ I_{pr3} = 184 A $\angle 240^o$ Secondary currents are I_{sek1} = 645 A $\angle 0^o$, I_{sek2} = 645 A $\angle 120^o$, I_{sek3} = 645 A $\angle 240^o$

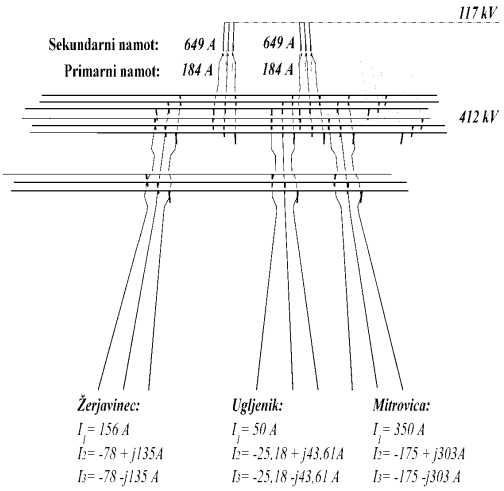

Fig. 10 Currents distribution for magnetic field computation

E. Magnetic Flux Density Inside TS 110 kV

The spatial distribution of the magnetic field inside TS 110 kV is shown in Fig. 11. All computations have been conducted for an observation surface 1,5 m above the ground.

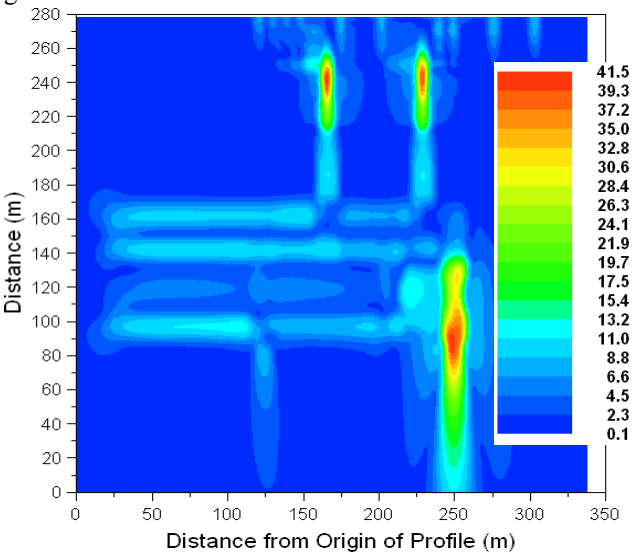

Fig. 11 Computed values for flux density B for plane 2m over ground

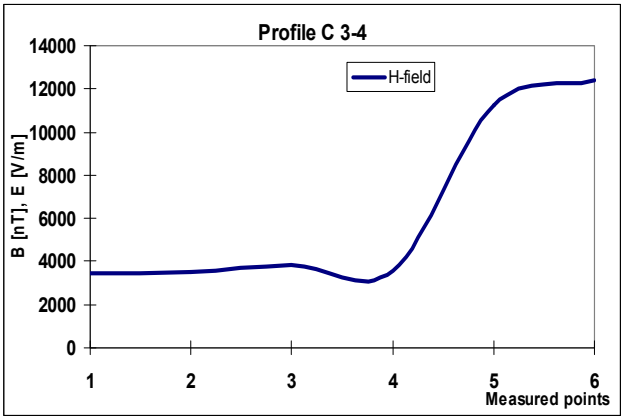

Fig. 12 Measured values for flux density B at profile C3-4

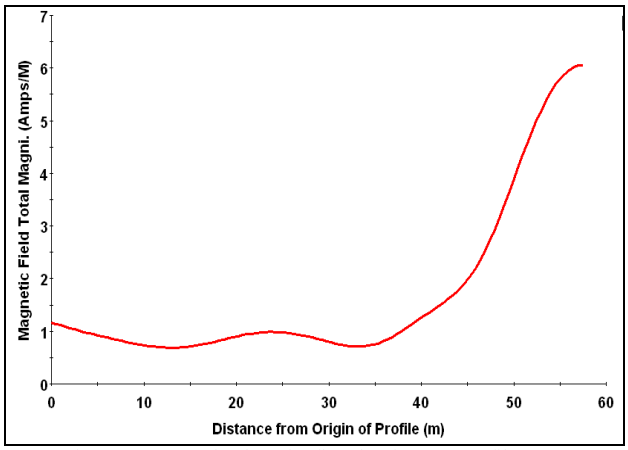

Fig. 13 Computed values for flux density B at profile C3-4

The permissible level for the magnetic density (B) in transformer station is 100 μT.

Table 5 Measurements of magnetic field at profile T1/110

Time [day]	Date [day]	H-Field X [nT]	H-Field Y [nT]	H-Field Z [nT]	H-Field 3D [nT]
11:48	15.7.2008	27900	29650	30100	50631,44
11:48	15.7.2008	34900	14215	20200	42756,48
11:49	15.7.2008	10090	9345	4520	14476,45
11:49	15.7.2008	2730	6130	2120	7037,34

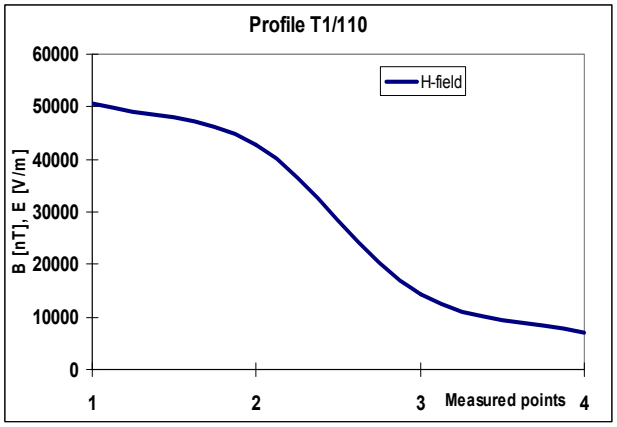

Fig. 14 Measured values for flux density B on profile T/110

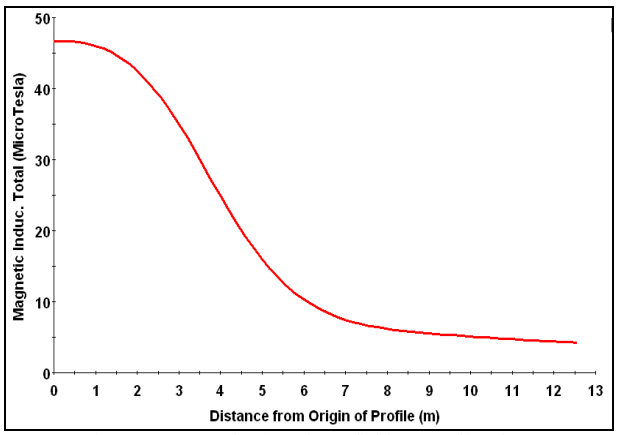

Fig. 15 Computed values for B field on profile T/110

Computed and measured values of flux density B are in good correlation.

Permissible levels of electrical field intensity E are overreached at some points for seven measured profiles C0-1, C3-4, C4-5, C8-9, C9-10, T1/400, T2/400.

Permissible levels of electrical field intensity E are not reached at profiles C7-8, UOG, UPS, T1/110 i T2/110.

In the parts of the transformer station where permissible levels of electric field intensity E are overreached, recommended duration of working personnel activities is less than 3 hours of permanent occupation.

In Fig. 16 and 17, some discrepancies between the computed and measured values, which could explain that current distribution in modeled transformer station do not reach real current distribution of real system, can be seen.

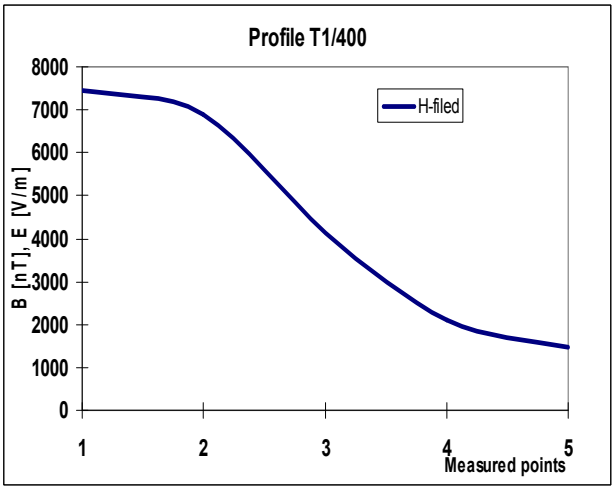

Fig. 16 Measured values for B field at profile T/400

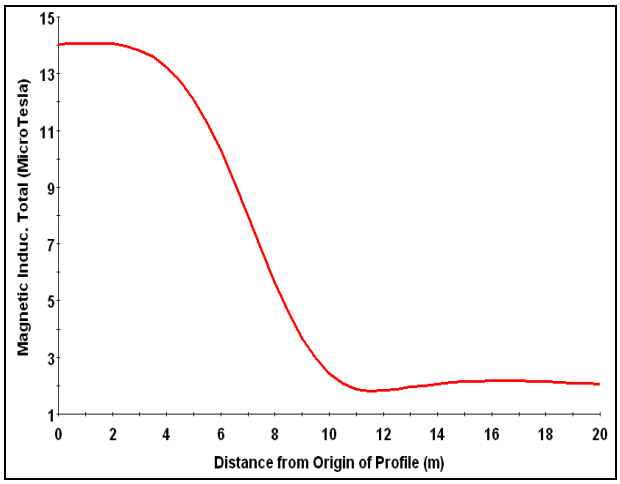

Fig. 17 Computed values for B field at profile T/400

V. Conclusion

High values of electromagnetic field can cause deleterious effects on humans exposed to them, so there is a need and obligation to compute and measure them. This paper presented a sample case of computation and measurements of electric field intensity (E) and magnetic field density (B) in a high voltage power transformer station TS 400/110 kV. Simulations were performed using CDEGS software (HIFREQ module) for an observation plane at 2 m over the ground. Measurements were performed using Maschek ESM-100 fieldmeter.

Several areas and profiles in the substation have overreached the permissible values for the electric field intensity 5000 (V/m), especially under the 400 kV busbars in the substation. The time spent in these areas needs to be less than 3 hours. Regarding the magnetic field density, the whole region is under the allowed levels (100 μT).

Acknowledgment

The authors gratefully acknowledge the contributions of Nina Mitskevitch PhD from SES technologies ltd. Canada for her work on the original version of this document.

References

[1] Z. Haznadar, Ž. Štih, *Electromagnetism 1 i 2*, Školska knjiga, Zagreb 1997

[2] T. Barić, S. Nikolovski, *Influence of conductor segmentation in grounding resistance calculation using boundary element method,* Proceedings from PIERS (Progress in Electromagnetic Research Symposium), Pisa-Italy, 28.-31. 03. 2004

[3] S. Nikolovski; D. Šljivac; M, Jinxi; *Electromagnetic field produced by overhead power lines,* Proceedings of the 8th International Conference on Operational Research KOI 2000 Hunjak, T., Scitovski, R. (ur.), Osijek : Zavod za matematiku Sveučilišta u Osijeku, 2000

[4] Zijad Haznadar and Željko Štih, *Electromagnetics fields waves and numerical methods,* IOS Press, Ohmsha, Amsterdam, ISBN: 1383-7281, Volume 20, 2000

[5] A. Selby and F. P. Dawalibi, *"Determination of current distribution in energized conductors for the computation of electromagnetic fields",* IEEE Transactions on Power Delivery, Vol. 9, No. 2, April 1994, pp. 1069-1078

[6] F. P. Dawalibi and A. Selby, *"Electromagnetic Fields of Energized Conductors," I*EEE Transactions on Power Delivery, Vol. 8, No. 3, July 1993, pp. 1275-1284

[7] F. P. Dawalibi and F. Donoso, *"Integrated analysis software for grounding, EMF, and EMI*," IEEE Computer Applications in Power, Vol. 6, No. 2, April 1993, pp. 19-24

[8] CDEGS User manual, SES technologies, Montreal, 2005

[9] Z.Haznarad, Ž. Štih, S. Berberović, B. Trkulja: "Computation of EMF in TS 400/110 kV Ernestinovod", FER Zagreb, October 2004